U5D: A 5 Dimensional Universe Model

A Geometrically Locked Late-Time Benchmark: No Free Dark-Sector Parameters, with a Falsifiable $\Sigma<1$ Lensing-Slip Prediction

Vahap Ünalan

mail@vahapunalan.com · 11.07.2026 · İstanbul

About the Author

I am an Electronics and Communications engineer with 35 years of experience.

Much as engineers map terrain with a theodolite, I independently analysed the published measurements of large sky surveys — supernova brightnesses, BAO distances, weak-lensing and growth statistics — covering roughly 160 million galaxies and quasars in total (DESI DR2, KiDS, DES-Y3, HSC and others).

Months of computation and model comparison led to the pixel-and-universe model presented here; this paper documents the current state of a year-long research effort.

Abstract

We present a cosmological model that treats the observable universe as an S^3 three-brane inside a five-dimensional bulk (four spatial dimensions plus time) and locks the dark sector to a single pixel geometry, whose core constant is $\eta = 5/\sqrt{27} = 0.96225$.

The matter fraction $\Omega_{cb} = 3/\pi^2$, the baryon fraction $\Omega_b = \pi/64$ and the dark-energy trajectory $w(a)$ are fixed by geometric prescriptions of the same construction ($w_0 = -\eta^2$ follows from a single projection postulate; w_a is a phenomenological residual). Only four standard parameters are left free: H_0, τ, n_s and A_s.

The prediction motivated by the geometry is a gravitational slip for light, $\Sigma(z) < 1$, with amplitude $A_\Sigma = 1-\eta \approx 3.8\%$.

The minimal model containing it (U5Ds; standard matter growth, $\mu = 1$) yields $\Delta\chi^2 = -9.84$ relative to ΛCDM over 19 observational likelihood blocks; the most developed version, which adds a growth slip of the same geometric amplitude (U5Dws; $\mu < 1$), reaches $\Delta\chi^2 = -13.16$.

The coefficient of this growth slip is fixed neither by the theory nor by current data (Section 7).

This preference arises entirely from two S8-tension-sensitive observations — the weak-lensing S8 priors and the growth rate $f\sigma 8$ — which enter as compressed, largely ΛCDM-derived priors and cannot be separated from baryonic feedback.

Restricted to the robust geometric probes (supernovae, BAO, CMB and H_0), the models show no such preference. The single sharp, falsifiable prediction is therefore $\Sigma(z) < 1$, and its primary test is Euclid's forthcoming tomographic weak-lensing measurement.

Keywords: dark energy · gravitational slip (μ, Σ) · braneworld · CPL · S8 tension · Euclid · discrete spacetime / pixel · parameter economy

1. Introduction

ΛCDM describes dark energy and dark matter with six free parameters. In this work we address the inverse question: rather than leaving these quantities free, if we lock them to a single geometric structure, how far can we go against the observations?

The aim is not a new detection but the construction of a highly-constrained, falsifiable benchmark. The distinguishing feature of the framework is that it builds the universe up from its smallest unit — a discrete Planck-scale 'pixel'.

The idea of discrete spacetime is not new (loop quantum gravity, causal-set theory); the originality here is the specific polytope structure of the pixel and the single constant that arises from it.

2. Geometric framework

The pixel consists of a 4-simplex (5-cell) core at the center and five surrounding channels (16-cell). The ratio of the norm of the five inner channels (5) to the norm of the reference volume ($\sqrt{27}$) gives the core constant: $\eta = \cos\theta_U = 5/\sqrt{27}$, $\theta_U = 15.79°$ ($\tan\theta_U = (\sqrt{2})/5 \approx 0.283$).

From this follow $\eta^2 = 25/27$ and the void fraction $1-\eta = A_\Sigma = 0.0377$; this void is the common-bulk volume outside the five channels. η is a minimality construction — a norm-ratio fixed by the pixel structure, not derived from a fundamental action (Section 9).

It can be written compactly as $\eta = h(A_4)/\lambda_1(S^3)^{3/2} = 5/3^{3/2}$, a form that records its two structural inputs (the Coxeter number $h(A_4) = 5$ and $\lambda_1(S^3) = 3$) rather than deriving them.

Its origin is geometric: η is the ratio of the norm of the unit volume filled by the five inner channels ($\sqrt{25} = 5$) to the norm of the reference volume arising from the pixel's $\sqrt{3}$ spatial diagonal ($\sqrt{27} = 3^{3/2}$) — not a fitted number but a norm-ratio fixed by the construction (though not derived from a fundamental action; Section 9).

These two norms rest on two structural axioms: 5 is the minimal number of positive vertices spanning a four-dimensional inner frame (d+1); $\sqrt{2}$ is the 16-cell edge length — the distance between adjacent vertices $\pm e_i$ of the spatial cross-polytope. η is thus a strongly-motivated construction — not a final derivation from a fundamental action (Section 9).

3. Locking of the dark-sector parameters

The dark sector contains no free parameters:

Quantity	Formula	Value
Baryon+CDM Ω_cb	$3/\pi^2$	0.30396
Total matter Ω_m = Ω_cb+Ω_ν	—	≈0.3054
Baryon Ω_b	$\pi/64$	0.04909
Dark energy w_0	$-\eta^2$	−0.92593
w_a (CPL)	$-(\eta^{-2}-\eta^2)$	−0.15407
U5D variant (constant w)	$-\eta$	−0.96225

In the dynamical variant w(a) crosses the phantom boundary (w = −1) at $z^* = \eta^2 \approx 0.93$; as a→0, $w \to -\eta^{-2} = -1.08$. The direction matches the dynamical dark energy ('quintom-B') favored by DESI DR2 (DESI Collaboration 2025; Lodha et al. 2025), with a weaker amplitude.

$\Omega\_cb = 3/\pi^2$ is a spectral anchor (the first Laplacian eigenvalue on S^3, $\lambda_1 = 3$); the rival candidate $\pi^2/32 = 0.308$ falls behind on the full data set (from the chains: 14887.19 − 14884.81 = +2.38).

When Ωm is left free the data prefer Ωm = 0.3071 ± 0.0013 — within ~1.3σ of the derived total corresponding to the locked value (≈0.305); the geometric lock is consistent with the data-adapted value.

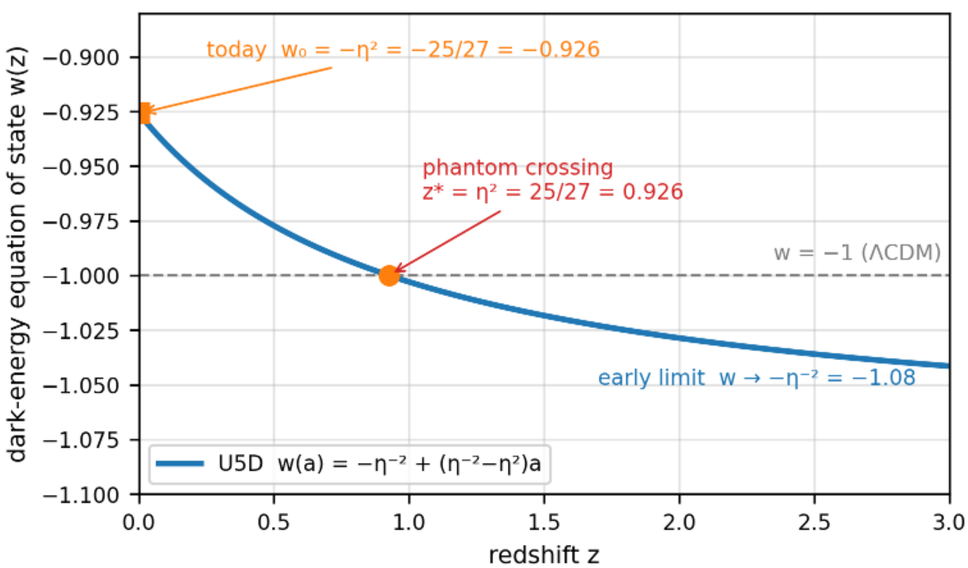

Figure 1. U5D dark-energy equation of state w(z): it crosses the phantom boundary (w = −1) at $z^* = \eta^2 = 25/27 = 0.926$; today $w_0 = -0.926$, in the early universe $w \to -\eta^{-2} = -1.08$.

The geometric origin of the other constants is likewise unique: $\Omega_{cb} = 3/\pi^2$ is adopted as a fixed spectral-geometric ansatz motivated by the first Laplacian eigenvalue on S^3 ($\lambda_1 = 3$); a full derivation connecting this spectral quantity to the Friedmann density parameter remains open (Section 9).

$\Omega_b = \pi/64$ is the product of the ratio of the active pixel's 4-ball volume to the hypercube volume ($\pi^2/32$) and the ratio of the radius to the circumference ($1/2\pi$): $(\pi^2/32)(1/2\pi) = \pi/64$. $w_0 = -\eta^2$ arises from the dark-energy pressure seeing the rank-2 (area) projection of η. $w_0 = -\eta^2$ is not an independent CPL parameter.

The single dynamical assumption of the theory is this: the pixel's W-void couples to the observable channels through the θ_U-projection — the lensing-slip, being a length-type (rank-1) channel, sees the void as $(1-\eta)$, while the pressure, being an area-type (rank-2) channel, sees it as $(1-\eta^2)$.

$\Sigma(0) = \eta$ and $1+w_0 = 1-\eta^2$ are the two outputs of this SINGLE projection postulate and cannot be tuned independently. The algebraic consequence $(1+w_0)/(1-\Sigma(0)) = (1-\eta^2)/(1-\eta) = 1+\eta = 1.962$ is a parameter-free internal-consistency test checkable by independent measurement of the two channels.

This structure removes w_0 from being a data-fitted freedom (zero free dark-sector parameters); however it is not a first-principles derivation — the projection postulate itself (including the rank assignments) is a fundamental assumption of the theory, and its derivation from a 5D action is an open problem.

The w_a trajectory rests on an additional volume argument and is labeled a phenomenological residual. $\Omega_b = \pi/64$, on the other hand, is a secondary lock — it is not as strongly motivated as $\Omega_{cb} = 3/\pi^2$ and the main claim does not rest on it.

Background and perturbation conventions. The expansion history uses the CPL form $w(a) = w_0 + w_a(1-a)$ (Chevallier & Polarski 2001; Linder 2003), with $\rho_{DE}(a)/\rho_{DE0} = a^{-3(1+w_0+w_a)} \exp[-3w_a(1-a)]$, so that $E^2(a) = \Omega_r a^{-4} + \Omega_m a^{-3} + \Omega_{DE} a^{-3(1+w_0+w_a)} \exp[-3w_a(1-a)]$.

Linear perturbations use the (μ, Σ) parametrization $k^2\Psi = -4\pi G a^2 \mu(a) \rho\Delta$ and $k^2(\Phi+\Psi) = -8\pi G a^2 \Sigma(a) \rho\Delta$, with μ and Σ taken scale-independent. Neutrinos are standard: $\Sigma m_\nu = 0.06$ eV (normal hierarchy), $N_{eff} = 3.044$, giving $\Omega_\nu \approx 0.0014$ and a total matter fraction $\Omega_m = \Omega_{cb} + \Omega_\nu \approx 0.3054$.

The S^3 structure is used as a spectral-geometric reference; the present likelihood implementation assumes a spatially flat FLRW background ($\Omega_k = 0$).

4. Gravitational slip: the Σ<1 prediction and an optional growth slip

The void fraction $1-\eta$ is a geometric capacity measure. We phenomenologically attribute the resulting gravitational slip to an effective projected bulk-Weyl anisotropic stress $E_{\mu\nu}$ (Shiromizu, Maeda & Sasaki 2000) and impose the corresponding closure as a boundary-condition ansatz. The lensing potential seen by light and the attraction felt by matter then scale differently:

$\Sigma(z) = 1 - A_\Sigma \cdot L(z)$ [lensing — the core prediction, common to all variants] ; $\mu(z) = 1 - \kappa \cdot A_\Sigma \cdot L(z)$ [growth]

Here $L(z) = \Omega_{DE}(z)/\Omega_{DE0}$ and κ is the growth-slip coefficient (Pogosian & Silvestri 2016). Today $\Sigma(0) = \eta = 0.962$; at high redshift the slip converges to the GR value 1. The minimal model fixes only the light slip and sets $\kappa = 0$ ($\mu = 1$, U5Ds).

The geometric closure suggests $\kappa = 4/3$ (U5Dws), for which $\mu(0) = 0.950$ — but this coefficient is not derived from the theory and is not identified by current data (Section 7). We restrict the phenomenological sector to luminal tensor propagation ($\alpha_T = 0$), consistent with GW170817, and do not include a Gauss–Bonnet interaction.

Internal consistency of the lensing channel: $(1+w_0)/(1-\Sigma(0)) = (1-\eta^2)/(1-\eta) = 1+\eta = 1.962$.

In potential language, the $\kappa = 4/3$ closure is equivalent to the time potential being suppressed twice as strongly as the space potential ($s_\Psi = 2\, s_\Phi$; $s_\Psi : s_{Weyl} : s_\Phi = 4:3:2$); this is an algebraic restatement of the assumed boundary condition, not a microscopic derivation.

A derivation of this ratio from the bulk-Weyl boundary problem remains open and is left to a separate technical study (Section 9).

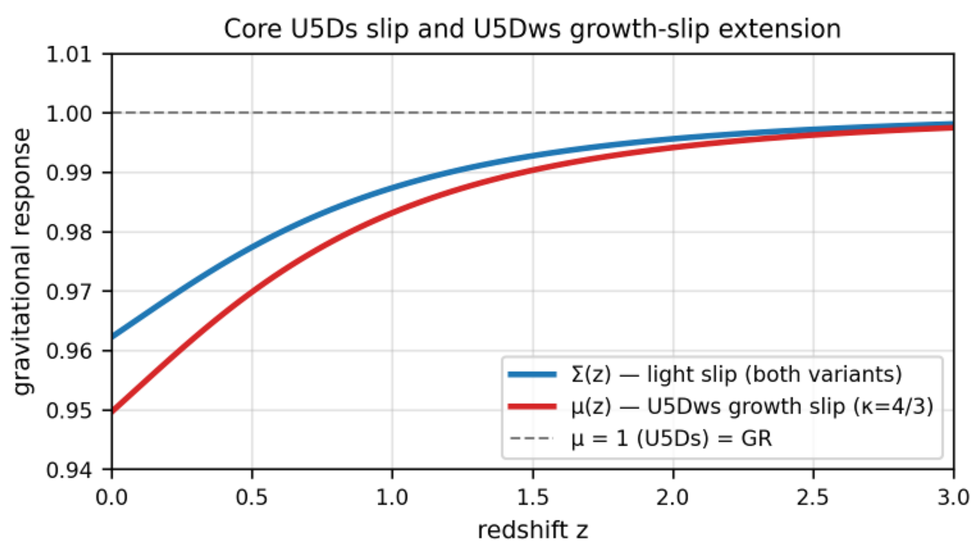

Figure 2. Gravitational slip: Σ(z) (lensing) and μ(z) (growth). With amplitude $A_\Sigma = 1-\eta$, today $\Sigma(0)=0.962$, $\mu(0)=0.950$; at high z both converge to the GR value of 1.

5. Substrate geometry

The following are motivational combinatorial facts about the substrate; deriving the cosmological parameters from them is an open problem (Section 9). Two action-independent combinatorial results support the micro-picture.

Regge angle-deficit: since the dihedral angle of the 16-cell is 120°, the channels tile flat E^4 with no deficit; since the dihedral angle of the 5-cell is arccos(¼) = 75.52°, the core carries a 57.91° deficit (curvature) at 4×75.52° = 302.09°.

W-B-B-B combinatorics: of the pixel's 8 boundary vertices 6 are spatial (light), 2 are W-directed; every three-dimensional boundary cell contains exactly one W vertex (B-B: 12, B-W: 12, W-W: 0).

6. Data and method

The analysis was carried out with Cobaya (Torrado & Lewis 2021). 19 likelihood blocks were combined in a common set: Planck NPIPE CamSpec (high-ℓ), Planck low-ℓ TT/EE and lensing, ACT DR6 lensing, SPT-3G 2022, BICEP/Keck 2018; Pantheon+ supernovae; DESI DR2 and SDSS DR16 BAO; cosmic chronometers; the 63-point fσ8 compilation; KiDS-1000, DES-Y3, HSC-Y3 weak-lensing S8 priors; eROSITA cluster-S8; SH0ES/JWST H_0.

These last five (KiDS/DES-Y3/HSC/eROSITA S8 and SH0ES/JWST H_0) are not full likelihoods but compressed (Gaussian) priors on the published, largely ΛCDM-derived S8/H_0 values (Asgari et al. 2021; Abbott et al. 2022; Dalal et al. 2023); used here as a pre-screen, they require a model-consistent cosmic-shear/cluster re-analysis for confirmatory inference (future work).

Each model was run on the same set with the Gelman–Rubin criterion $R-1 < 0.05$.

The growth effect of the gravitational slip ($\mu<1$) was applied to the fσ8 observation via a suppression kernel derived from a validated linear-growth solution; an independent MGCAMB computation (Zhao et al. 2009; Hojjati et al. 2011) gave the same magnitude (≈2.3% suppression in fσ8).

The total χ^2 was taken only from the leaf-likelihood values; including block subtotal columns roughly doubles the sum and was not used.

Table. The 19 likelihood blocks, their type and the observational sample each rests on. The weak-lensing / cluster / H_0 entries enter as compressed priors on published values. In total the constraints draw on ≈160 million galaxies and quasars — dominated by the imaging surveys DES-Y3 (≈100 M), HSC (≈25 M), KiDS (≈21 M) and DESI DR2 (≈14 M) — together with ≈1,550 supernovae, ≈5,300 clusters and all-sky CMB.

Data block	Type	Observational sample
Planck NPIPE + low-ℓ + lensing	full likelihood	CMB (all-sky)
ACT DR6, SPT-3G, BICEP/Keck	full likelihood	CMB (wide-field)
Pantheon+ supernovae	full likelihood	≈1,550 SNe Ia
DESI DR2 BAO	full likelihood	≈14 M galaxies + quasars
SDSS DR16 Lyα (auto+cross)	full likelihood	≈0.21 M Lyα quasars
Cosmic chronometers	full likelihood	≈32 H(z) points
fσ8 (KP2018)	compiled likelihood	63 RSD points
KiDS-1000 S8	compressed prior	≈21 M galaxies
DES-Y3 3×2pt S8	compressed prior	≈100 M galaxies
HSC-Y3 S8	compressed prior	≈25 M galaxies
eROSITA cluster S8	compressed prior	≈5,300 clusters
SH0ES / JWST H_0	compressed prior	Cepheid/TRGB calibrators

7. Results

Same-set model ladder on the full data set:

Model	k	χ^2	$\Delta\chi^2$ vs ΛCDM
U5Dws (w(a); Σ<1, μ<1)	4	14884.81	−13.16
U5Ds (w(a); Σ<1, μ=1)	4	14888.13	−9.84
w0waCDM (free w_0, w_a)	8	14890.73	−7.24
U5Dw (w(a); no slip)	4	14893.81	−4.17
wCDM (free w)	7	14897.22	−0.75
U5D (constant w=−η; no slip)	4	14897.96	−0.02
ΛCDM (w=−1; no slip)	6	14897.97	0

Note: $\Delta\chi^2$ is computed from the exact chain values; since the χ^2 column is rounded to two decimals, individual differences may vary by ±0.01. ΔBIC = $\Delta\chi^2$ + Δk·ln N with N ≈ 1.52×10^4 effective data points (ln N = 9.63). Because the geometric locks and model variants were developed using overlapping datasets, this comparison is not an out-of-sample confirmation; the prospectively-fixed quantity is the future lensing-slip amplitude (Section 8), registered with the public archive date.

Table. Best-fit χ^2 per likelihood for all seven models on the same 19-likelihood data set. Along the progression ΛCDM → U5D (static) → U5Dw (w(a)) → U5Ds (Σ<1) → U5Dws (Σ<1,μ<1) the gain builds up in the growth (fσ8) and weak-lensing S8 channels; wCDM and w0waCDM are the standard free-w comparisons, and U5D (static w=−η) ≈ ΛCDM. Rows are rounded; column totals match Table 1.

Likelihood	ΛCDM	wCDM	w0waCDM	U5D	U5Dw	U5Ds	U5Dws
Planck low-ℓ TT	22.11	22.48	22.21	22.14	22.44	22.52	22.53
Planck low-ℓ EE	395.94	396.09	395.70	396.73	396.05	397.09	397.21
Planck lensing	10.38	10.28	10.23	10.97	10.29	9.60	9.48
Planck NPIPE	10550.33	10551.17	10549.91	10552.72	10552.09	10551.22	10551.23
ACT DR6	16.43	16.60	16.42	17.25	16.64	15.76	15.60
BICEP/Keck	538.63	538.65	538.64	538.84	538.73	538.47	538.43
SPT-3G	1876.25	1876.16	1875.84	1876.34	1876.54	1876.66	1876.74
Pantheon+	1406.42	1404.30	1403.00	1403.06	1402.67	1402.67	1402.67
DESI DR2	10.59	10.88	9.20	10.70	9.25	9.25	9.25
SDSS Lyα-auto	1.39	1.47	1.07	1.53	1.33	1.33	1.33
SDSS Lyα×QSO	2.80	2.90	2.35	2.98	2.72	2.72	2.72
SH0ES M_B	0.01	0.10	0.00	0.00	0.02	0.00	0.03
Chronometers	14.83	14.83	15.01	14.85	14.84	14.84	14.84
fσ8 (RSD)	39.92	37.98	35.68	35.89	36.00	37.04	33.78
KiDS-1000	2.79	2.88	3.41	2.62	2.90	0.53	0.57
DES-Y3	1.90	1.98	2.51	1.73	2.00	0.07	0.09
JWST H_0	4.21	5.33	6.36	6.38	6.11	6.11	6.11
eROSITA	2.26	2.31	2.17	2.49	2.35	2.11	2.07
HSC-Y3	0.80	0.83	1.00	0.75	0.83	0.12	0.13
Total (19)	14897.97	14897.22	14890.73	14897.96	14893.81	14888.13	14884.81

U5Dws gives the best fit with four free parameters (nominal ΔBIC ≈ −32 under the adopted data-count convention; see the note below). The source of this preference is determined by the channel decomposition.

In the μ = 1 version (U5Ds) most of the advantage comes from the three weak-lensing S8 priors (KiDS, DES, HSC together ≈ −5.0); the supernova, BAO, chronometer and H_0 channels do not change.

When μ < 1 is added (U5Dws), most of the extra −3.3 is in the growth channel: the fσ8 contribution drops from 36.0 to 33.8 (−2.2); the remaining ≈ −1.1 consists of small shifts within the soft channel, and no other channel changes by more than 0.2.

When fσ8 is removed entirely (18 likelihoods), the dynamical model without slip is practically indistinguishable from ΛCDM ($\Delta\chi^2 \approx -0.06$) — independently confirming the gain map. The geometric postulate fixes only the light slip (Σ<1); the minimal model containing it is U5Ds ($\Delta\chi^2 = -9.84$).

The coefficient κ of the growth slip is pinned neither by the theory ($r = s_\Psi/s_\Phi = 2$ is not derived) nor by current data (the κ-profile is flat at current sensitivity: κ = 1 and κ = 4/3 are indistinguishable; a full joint MCMC is planned).

The best fit of U5Dws (−13.16) is therefore an upper-bound variant; the main result is the geometry-motivated Σ(z) < 1 prediction.

Table. Posterior means and 68% intervals (converged chains, 30% burn-in). For U5Dws the dark-sector fractions are locked, so H_0, τ, n_s, A_s are the only free parameters. The background $S_8 \approx 0.80$ stays close to ΛCDM: the model matches the low weak-lensing S_8 through the slip Σ<1, not a shifted σ_8.

Parameter	ΛCDM	U5Dws
H_0 [km/s/Mpc]	68.50 ± 0.22	67.66 ± 0.04
Ω_m	0.298 ± 0.003	0.3054 (locked)
σ_8	0.801 ± 0.004	0.795 ± 0.003
$S_8 = \sigma_8\sqrt{(\Omega\_m/0.3)}$	0.798 ± 0.006	0.802 ± 0.004
n_s	0.9702 ± 0.0024	0.9700 ± 0.0019
τ	0.054 ± 0.005	0.058 ± 0.004
$\ln(10^{10}$ A_s)	3.042 ± 0.009	3.050 ± 0.009
Gelman–Rubin R−1 (means)	0.026	0.028
Effective samples	≈37,000	≈27,000

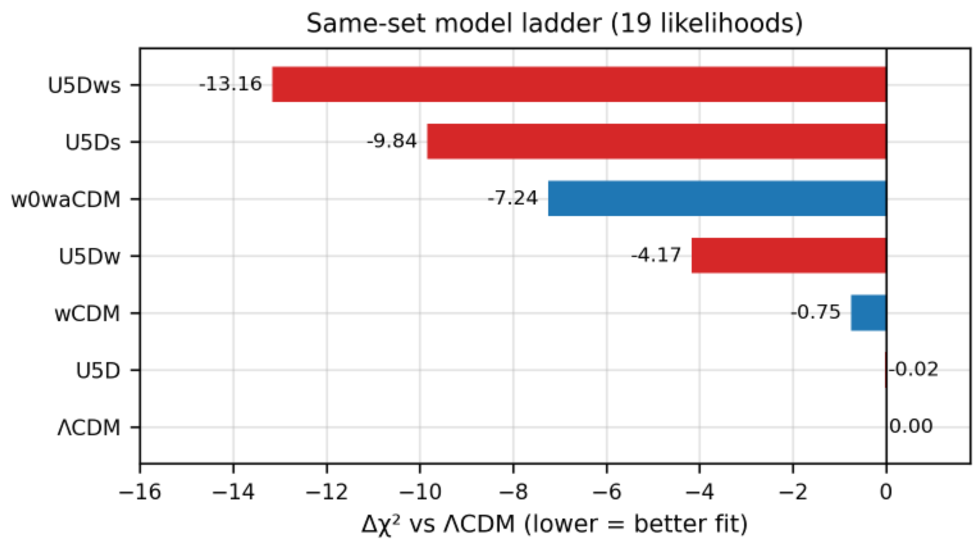

Figure 3. Same-set χ^2 ladder (19 likelihoods), relative to the ΛCDM baseline: U5D → U5Dw → U5Ds → U5Dws. U5Dws $\Delta\chi^2 = -13.16$.

Table. Position of U5D among modified-gravity families.

Model	Free DE par.	w(a)	Σ	μ	Distinguishing
ΛCDM	0	−1	1	1	baseline
Quintessence	1+	>−1	1	1	no slip
Horndeski	functions	free	varies	varies	free functions
DGP / nDGP	1	≈−1	≈1	>1	μ>1 (opposite sign)
U5D	0	η-locked	<1	1→<1	η-lock; Σ<1 (& μ<1)

These two observations — weak-lensing S8 and fσ8 — are sensitive to the S8 tension, and the low S8 value cannot be disentangled from baryonic feedback: the ≈2.8% lensing suppression at Σ(z=0.3) overlaps with the typical baryonic-feedback range (2–5%) (van Daalen et al. 2011, 2020).

To separate whether the advantage comes from genuine expansion geometry or from this tension-sensitive channel, a run was performed with weak-lensing and fσ8 removed, using only the robust probes — supernovae, BAO, CMB, cosmic chronometers and H_0 (14 likelihoods):

Model	**$\Delta\chi^2$ (full, 19-lik)**	**$\Delta\chi^2$ (robust, 14-lik)**
ΛCDM	0	0
U5Ds	−9.84	+1.7
U5Dws	−13.16	+1.6

Restricted to the robust set, the U5Dws advantage collapses: relative to a re-optimized ΛCDM on these fourteen likelihoods, U5Dws and U5Ds sit at $\Delta\chi^2 \approx +1.6$ and +1.7 — that is, no preference. The channel decomposition explains why.

U5Dws fits the expansion data better (supernovae −3.8, BAO −1.5), but this is offset by small CMB (+1.2) and local-H_0 (+1.9) penalties; and because the geometry is locked, the model cannot re-optimize these channels the way ΛCDM can.

The full-data −13.16 therefore originates entirely in the tension-sensitive soft channel, and the information-criterion advantage reflects parameter economy rather than a superior fit.

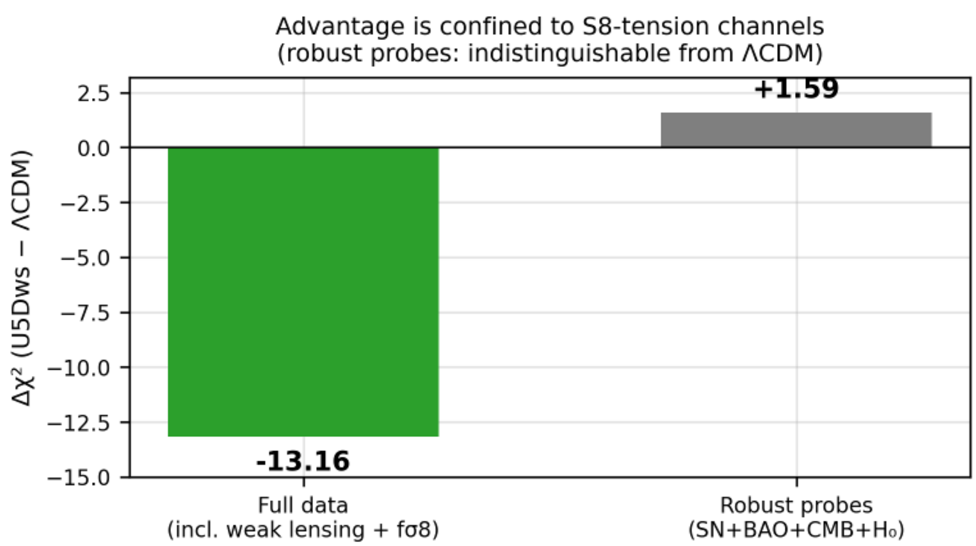

Figure 4. Channel decomposition of the −13.16: restricted to the robust probes (SN+BAO+CMB+H_0) the preference vanishes ($\Delta\chi^2 \approx +1.6$, i.e. ≈ ΛCDM); the entire gain comes from the S8-sensitive soft channel (weak-lensing S8 + fσ8).

8. Falsifiable prediction and Euclid

The model's locked, sharp prediction is $\Sigma(z) < 1$ ($A_\Sigma = 1-\eta$). The gravitational slip produces a probe-type-dependent S8 ordering: weak-lensing < CMB-lensing < RSD.

The present offset is $\Delta S8 \approx -0.010$; forthcoming tomographic weak-lensing (Euclid plus SO/Advanced-SO CMB-lensing combinations; Euclid Collaboration 2025) can test this at the ~1.5 –2σ level.

The distinguishing signature is this: in the U5Ds limit ($\mu = 1$) growth remains approximately standard while lensing is suppressed; in the U5Dws version the same geometric amplitude is also transferred to the growth channel as a controlled suppression ($\mu(0) = 0.950$); in both cases $\Sigma < 1$ separates the model from a pure σ8-shift and from nDGP-type models that give $\mu > 1$.

The pre-registered falsification threshold is $|\text{offset}| < 0.005$; equivalently, the model is falsified if a tomographic measurement constrains the slip amplitude to $A_\Sigma = 0$ (GR), excluding $A_\Sigma = 1-\eta = 0.0377$ at high credibility.

A second falsifiability: if the independently-measured ratio $(1+w_0)/(1-\Sigma(0))$ deviates significantly from 1.962, the rank structure linking the two channels breaks.

With current KiDS-Legacy + ACT DR6 data a band-power pre-test is consistent with GR ($\chi^2/\text{dof} = 1.06$); at $A_\Sigma = 0.0377$, $\Delta\chi^2 = -2.08$; but since a σ8-free joint fit does not break the degeneracy, this is not a detection.

As a linear-regime consistency quantity, the ratio μ/Σ differs across the growth-slip variants ($1/\eta \approx 1.039$ for U5Ds, 1 for the isotropic $\kappa = 1$ case, ≈ 0.987 for U5Dws).

This may motivate future large-scale lensing–dynamics consistency tests, but its translation to individual cluster masses is not attempted here, as that would require a nonlinear completion of the theory (halo profile, screening, hydrostatic bias).

Table. Probe-dependent growth/lensing response in the two variants.

Observable	U5Ds (μ=1)	U5Dws (κ=4/3)
Cosmic shear (WL)	suppressed	suppressed
CMB lensing	integ. suppression	integ. suppression
RSD / fσ8	~standard	suppressed

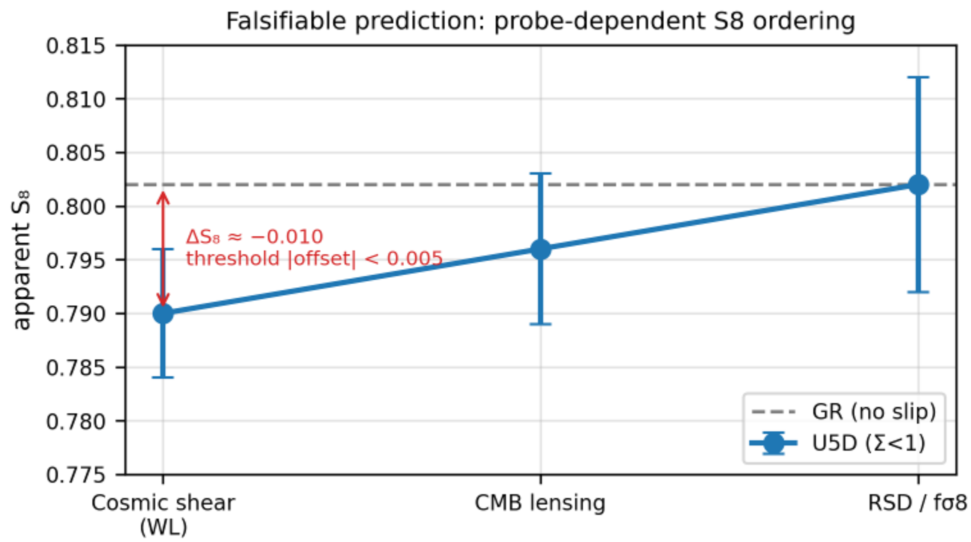

Figure 5. Falsifiable prediction: probe-type-dependent S8 ordering and the ΔS8 ≈ −0.010 offset; pre-registered threshold |offset| < 0.005. Euclid tomographic shear is the primary test. (Illustrative sensitivity target, not an official Euclid forecast.)

9. Limitations and open problems

(1) $\eta = 5/\sqrt{27}$ is not derived from a fundamental action; it is a construction resting on two structural axioms (inner-frame dimension $d+1 = 5$; Z^4 nearest-neighbor $\sqrt{2}$). η is also not a natural polytope invariant of the 5-cell+16-cell; it is a particular choice of norm-ratio. (2) $A_\Sigma = 1-\eta$ is a postulate.

(3) The fit-preference on the full data set comes from a channel degenerate with baryonic feedback; on the robust probes the model is indistinguishable from ΛCDM. (4) The model does not resolve the H_0 tension; since there is no preference for high Ω_m and the locked values incur a small CMB penalty, the tensions worsen slightly.

(5) The full Friedmann bridge for $\Omega_{cb} = 3/\pi^2$ is open; the S^3 choice gives $\lambda_1 = 3$ whereas RP^3 gives $\lambda_1 = 8$, and this choice has not been demonstrated.

(6) The w_a component of the dynamical trajectory is a phenomenological residual; $w_0 = -\eta^2$, on the other hand, is the output of the single projection postulate shared with the slip (not a first-principles derivation, Section 3).

An analytic pre-screen — applying a common free feedback amplitude to the three S8 priors — shows that this nuisance can absorb the shear channel (≈ −5) but not the fσ8/growth channel; a full joint MCMC is planned.

(7) μ and Σ describe only linear cosmological scales; the present framework does not define the local or nonlinear completion of the theory, so solar-system and PPN consistency (e.g. the Cassini bound) remains an open requirement rather than a demonstrated result.

(8) The ($\mu<1$, $\Sigma<1$) phenomenology is not a novel region — No-Slip Gravity (Linder 2018) and anisotropic-stress/viscous dark energy (Mota et al. 2007) share it; U5D's distinctiveness is not a new (μ, Σ) region but locking the whole dark sector to a single geometric constant (η).

10. Conclusion

U5D is a cosmological model with zero free dark-energy parameters that locks the dark sector to a single geometric constant. Its main result is a geometry-motivated falsifiable prediction: a light slip $\Sigma(z) < 1$ ($A_\Sigma = 1-\eta$), to be sharply tested by Euclid.

On the fit side, the minimal slip model (U5Ds) gives $\Delta\chi^2 = -9.84$ and the version adding a growth slip (U5Dws) −13.16 relative to ΛCDM; but this preference is entirely in the S8-tension-sensitive, baryon-degenerate channel, and on the robust probes the model is indistinguishable from ΛCDM.

The value of the model lies in two points: the parameter economy of locking the entire dark sector to a single number, and a locked $\Sigma(z) < 1$ prediction that can be sharply tested by Euclid. The first-principles derivation of η and Euclid's measurement will determine the model's future.

Author contribution and computational disclosure

The author developed the physical hypotheses and model architecture. AI systems assisted with coding, literature organization, numerical cross-checking and language editing. All scientific claims and released calculations remain the author's responsibility.

References

Abdul-Karim, M. et al. (DESI Collaboration), DESI DR2 Results II: Measurements of Baryon Acoustic Oscillations and Cosmological Constraints, Phys. Rev. D 112, 083515 (2025); arXiv:2503.14738. DR2 LyA BAO: arXiv:2503.14739.

Lodha, K. et al., Extended Dark Energy analysis using DESI DR2 BAO measurements, arXiv:2503.14743 (2025).

Brout, D. et al., The Pantheon+ Analysis: Cosmological Constraints, ApJ 938, 110 (2022); Scolnic, D. et al., ApJ 938, 113 (2022).

Planck Collaboration, NPIPE/PR4; Rosenberg, E., Gratton, S. & Efstathiou, G., CamSpec PR4 likelihood, MNRAS 517, 4620 (2022).

Madhavacheril, M. S. et al. (ACT), DR6 CMB lensing, ApJ 962, 113 (2024); SPT-3G Collaboration (2022); BICEP/Keck, BK18 (2021).

Alam, S. et al., eBOSS/SDSS DR16 cosmology, Phys. Rev. D 103, 083533 (2021).

Kazantzidis, L. & Perivolaropoulos, L., fσ8 growth compilation, Phys. Rev. D 97, 103503 (2018).

Asgari, M. et al., KiDS-1000 cosmic shear, A&A 645, A104 (2021); Abbott, T. M. C. et al., DES-Y3 3×2pt, Phys. Rev. D 105, 023520 (2022); Dalal, R. et al., HSC-Y3 cosmic shear, Phys. Rev. D 108, 123519 (2023).

Bulbul, E. et al., eROSITA eRASS1 cluster cosmology (2024); Riess, A. G. et al., SH0ES/JWST H0 (2024).

Shiromizu, T., Maeda, K. & Sasaki, M., The Einstein equations on the 3-brane world, Phys. Rev. D 62, 024012 (2000).

Chevallier, M. & Polarski, D., IJMPD 10, 213 (2001); Linder, E. V., PRL 90, 091301 (2003) — CPL.

Dvali, G., Gabadadze, G. & Porrati, M., PLB 485, 208 (2000) — DGP (comparison).

Pogosian, L. & Silvestri, A., What can cosmology tell us about gravity?, Phys. Rev. D 94, 104014 (2016).

Zhao, G.-B. et al., MGCAMB, Phys. Rev. D 79, 083513 (2009); Hojjati, A., Pogosian, L. & Zhao, G.-B., JCAP 08, 005 (2011).

Torrado, J. & Lewis, A., Cobaya, JCAP 05, 057 (2021); Lewis, A. & Challinor, A., CAMB (2000).

Berger, M., Laplacian spectrum on S^3 (1971); Coxeter, H. S. M., Regular Polytopes, Dover (1973).

Linder, E. V., No-Slip Gravity, Phys. Rev. D 97, 023518 (2018); arXiv:1801.01503.

Mota, D. F., Kristiansen, J. R., Koivisto, T. & Groeneboom, N. E., Constraining dark energy anisotropic stress, MNRAS 382, 793 (2007); arXiv:0708.0830.

Di Valentino, E. et al., Class. Quantum Grav. 38, 153001 (2021); Abdalla, E. et al., JHEAp 34, 49 (2022).

van Daalen, M. P. et al., MNRAS 415, 3649 (2011); van Daalen, McCarthy & Schaye, MNRAS 491, 2424 (2020); Schneider, A. & Teyssier, R., JCAP 12, 049 (2015) — baryonic feedback.

Euclid Collaboration, Q1 quick data release and mission overview (2025–2026).

Data and code availability: MCMC chains, Cobaya configurations and the slip/growth modules will be deposited in a versioned Zenodo archive upon release (DOI assigned at publication).

Note: the DESI DR2 arXiv identifiers have been verified (2503.14738 / 14739 / 14743); the remaining observational-reference identifiers were checked against their published records.